Strong regional trends in extreme weather over the next two decades under high- and low-emissions pathways

Article

Accepted Version

Unprecedented regional trends in extreme weather until 2040, even under strong mitigation

Carley E. Iles[1], Bjørn H. Samset[1], Marit Sandstad[1], Nina Schuhen[1], Laura J. Wilcox[2], Marianne T. Lund[1]

1. CICERO Center for International Climate Research, Oslo, Norway

2. National Centre for Atmospheric Science, Department of Meteorology, University of Reading, Reading, UK

Abstract

Global warming is rapidly shifting climate conditions away from what societies and ecosystems are adapted to. While the magnitude of changes in mean and extreme climate are broadly studied, regional rates of change, a key driver of climate risk, have received less attention. Here we show, using large ensembles of climate model simulations, that large parts of the tropics and subtropics, encompassing 70% of current global population, are expected to experience unprecedented (>2 standard deviations) joint rates of change in temperature and precipitation extremes combined over the next 20 years, under a high emissions scenario, dropping to 20% under strong emissions mitigation. This is dominated by temperature extremes, with most of the world experiencing unusual (>1 standard deviation) rates relative to the pre-industrial, but unusual changes also occur for precipitation extremes in northern high latitudes, Southern and Eastern Asia and equatorial Africa. However, internal variability is high for 20-year trends, meaning that in the near-term, trends of the opposite sign are still likely for precipitation extremes, and rare but not impossible for temperature extremes. We also find that rapid clean-up of aerosol emissions,

mostly over Asia, leads to accelerated co-located increases in warm extremes and influences the Asian summer monsoons.

Many aspects of the climate are currently entering conditions unprecedented in millennia[1]. The present sustained rate of global mean surface warming is also unprecedented in at least the last 2000 years[2–4]. Climate risk, and the ability of nature and society to adapt to these new conditions, depend critically on the local rates of change of mean and extreme conditions[5,6]. Whilst nature and society are accustomed to a certain amount of regional change, due to natural and internal variability of the climate system on various timescales, changes that occur faster than this can be expected to have particularly strong impacts. For instance, rapid changes increase the risk of unprecedented conditions and extreme events such as the record-shattering heatwave in the US Pacific Northwest in 2021, which was deemed impossible without climate change[7,8].

Extreme events further account for a disproportionate share of the realized impacts of climate change. For instance, heatwaves may cause heat stress and excess mortality of both people and livestock, stress to ecosystems, reduced agricultural yields, difficulties in cooling power plants, and transport disruption. Similarly, precipitation extremes can lead to flooding and damage to settlements, infrastructure, crops and ecosystems, increased erosion and reduced water quality[9]. Thus, society seems particularly vulnerable to high rates of change of extremes, especially when multiple hazards increase at once. There is also an increasing risk of compound events, where extreme conditions occur simultaneously or in succession, which can combine non-linearly to result in greater impacts than would be expected from the sum of each individual component[10,11]. The 2022 Pakistan floods were likely such an occurrence, where an early heat wave transitioned into an unprecedentedly wet monsoon season. Other examples include combined heat and drought, increasing the risk of wildfires and exacerbating impacts on crops and ecosystems, or the combination of storm surges, caused by strong onshore winds, and heavy inland precipitation, exacerbating coastal flooding[10,11]. Thus, if a region is projected to experience rapid rates of change in two or more types of extremes, then the rates and intensities of unprecedented compound events may also increase rapidly.

Nevertheless, sustained decadal rates of change under global warming remain little studied in comparison to absolute changes, such as average temperatures or changes to the return values of extreme events. For example, the recent IPCC 6th Assessment Report did not systematically assess regional rates of change beyond mean temperatures and precipitation, or include them as a dedicated indicator when quantifying climate risk[12]. Also, there is little literature available on how concurrent changes in multiple climate forcers, such as long-lived greenhouse gases and short-lived aerosol emissions, can combine to dampen or amplify regional rates of change on decadal scales.

Here we examine projected rates of change in temperature and precipitation extremes over the period 2021-2040 ('near-term'), and beyond, compared to pre-industrial rates and variability, using four large ensembles of CMIP6 climate model simulations (ACCESS-ESM1-5, EC-Earth3, CanESM5 and MPI-ESM1-2-LR; see Methods and Table S1). We focus on regional changes, due to their increased relevance to the experience of people and ecosystems compared to the global mean, and identify regions projected to experience substantial changes in rates of one or more extreme event index over the coming decades. The main novelty of our study is to quantify how current forced changes and internal variability interact and play out on a decadal time scale, for a set of commonly used indicators of change.

In the following, we first give examples of how near-term regional rates of change of extreme events are projected to accelerate beyond typical pre-industrial variability, even under strong mitigation of greenhouse gas and aerosol emissions, with a focus on areas with strong changes, high population, or both. We then analyse the joint near-term evolution of extreme temperatures and 5-day rainfall events and examine how much of the world's population will experience unprecedented rates in one or both indices[13–15]. Finally, we discuss how 20-year trends in both indices evolve through to 2080, and the influence of near-term aerosol emission changes on regional rates of change of extreme events.

Changes in rates for single extremes indices

In Figure 1, we show near-term (2021-2040) rates of change in the annual maximum of daily maximum temperature (TXx), and the amount of precipitation during the wettest 5-day period of the year (Rx5day), compared to the spread of 20-year trends in pre-industrial (PI) conditions. Results shown are from ACCESS-ESM1-5. We use this model for illustration, as it has results that are broadly representative of the multi-model results. ACCESS-ESM1-5 has an Equilibrium Climate Sensitivity (ECS) within the IPCC assessed range (3.9 °C; Methods), and jointly, our four models (shown in the supplement) broadly span the range. This includes a so-called "hot model", with an ECS of 5.6 °C (CanESM5). We show a selection of IPCC AR6 regions[16] where multiple models project clear changes in rates relative to the PI, prioritising those with high present-day population density (see Figure 2) and ensuring representation of all populated continents where we find clear changes (Methods). The remaining regions are shown in Figure S1 and S2.

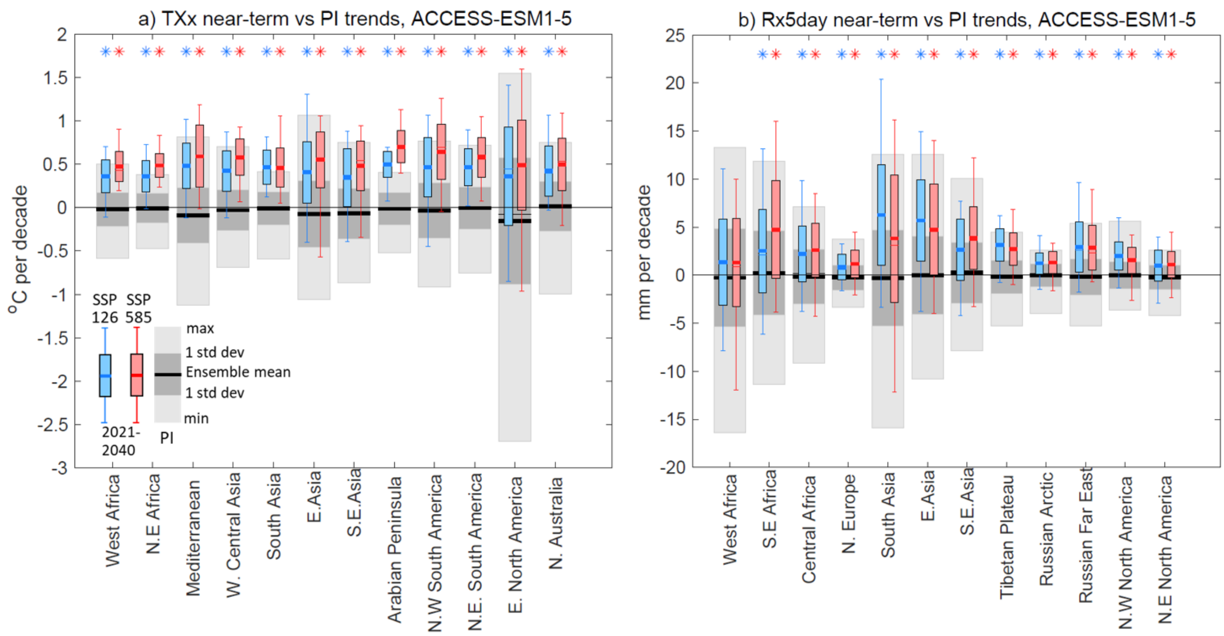

Figure 1: Near-term trends in extremes indices compared to pre-industrial trends. Trends in (a) TXx (°C per decade) and (b) Rx5day (mm per decade) for selected AR6 regions for 2021-2040 compared to 20-year trends in the pre-industrial period, as simulated by the ACCESS-ESM1-5 40-member large ensemble. For the near-term future, SSP1-2.6 is shown in blue, SSP5-8.5 in red, whilst the pre-industrial period (PI, defined as 1850-1900) is shown in grey. Ensemble mean (median) trends are shown with thick (thin) horizontal lines, the standard deviation spread across members is shown by the boxes for near-term, or dark grey shading for the pre-industrial, and the entire ensemble spread is shown with the whiskers or light grey shading respectively. Asterisks indicate whether the difference between PI and near-term trend distributions are significant based on a K-S test ($p<0.05$). Other models and regions are shown in Figures S1 and S2.

For TXx, we find very strong warm shifts in the near-term distribution of 20-year rates of change, relative to PI, across the ACCESS-ESM1-5 ensemble (K-S test, $p<0.05$, asterisks, see

Methods) for all regions in Figure 1a, and for both the high and low emission scenarios. Whilst larger changes relative to the PI can generally be seen in SSP5-8.5 compared to SSP1-2.6, significant changes in rate distributions can be seen in both scenarios and scenario differences are small compared to the overall ensemble spread. The other climate models show a similar overall pattern of results, although CanESM5 tends to show more distinct changes, whilst MPI-ESM1-2-LR shows less distinct changes (Figure S1). These results may reflect their differing climate sensitivities (see Table S1) in agreement with Smith et al., (2015)[4] and Chavaillaz et al. (2016)[15].

Figure 1b shows equivalent results for Rx5day. The regions of clear rapid change in extreme precipitation relative to PI trends tend to include the mid-to high northern latitudes, low latitude Asian and equatorial African countries. Differences in rates of change between the near-term and PI are less clear than for TXx, owing primarily to the higher variability of precipitation. Nevertheless, a significant shift towards wetter extremes is seen for both scenarios in all but one region shown (West Africa), with the near-term ensemble mean rate moving out of the PI standard deviation ensemble spread for at least one scenario (except for Central Africa). Note that the other large ensembles show much clearer changes in rates for West Africa and Central Africa (Figure S2). Scenario differences are also less distinct than for TXx, albeit with hints of stronger differences in regions where the two scenarios differ most strongly in their future aerosol emissions (Supplement). Statistically significant differences in trend distributions in Rx5day between the near-future and PI are also found in many other regions, almost always in a wettening direction (Figure S2).

We have also investigated rates of change of consecutive dry days (CDD); see Figures S23-26 and S10. Changes in rates are less clear than for TXx or Rx5day compared to pre-industrial trends, although statistically significant changes in trend distributions in CDD do occur in some regions.

Simultaneous changes in rates for multiple extremes

We now investigate the joint evolution of projected rates of change in both indices. The map in Figure 2 highlights regions undergoing substantial changes in joint rates of change for the near-future relative to the pre-industrial period. Specifically, regions are highlighted that experience a change in ensemble mean joint rates greater than two standard deviations (S.D.s) of pre-industrial trend variability in at least 3 out of 4 models (see Methods). This can be interpreted as a region very likely experiencing sustained, unprecedented rates of change for two or more decades, given that a 2+ standard deviation trend based on large ensembles has a low probability of having occurred over the single realisation of the real world with its limited sample size. Under SSP5-8.5, more than a third of land regions experience joint changes >2 S.D.s for the 2021-2040 period. The regions are clustered at lower latitudes, and often contain low-income countries that are particularly vulnerable to the impacts of climate change, exacerbating the climate risk from this compound hazard. Southern Asia and the Arabian Peninsula are projected to see these unprecedented joint changes also under SSP1-2.6. If we weaken the criterium to one standard deviation of PI variability, almost all regions experience such joint near-term changes under SSP5-8.5, and most also under SSP1-2.6 (Figure 3f).

The scatterplots in Figure 2 show regional mean near-term rates of changes in TXx vs Rx5day for ACCESS-ESM1-5. To illustrate the influence of internal variability, we include all ensemble members, as well as the ensemble mean and standard deviation spread, and how this compares to the 1 and 2 standard deviation spread of PI rates of change (ellipses, see Methods). The regions shown are those having clear joint changes in the central map, prioritising those with high population, and ensuring at least one region per continent is selected (the rest are shown in Figure S5). In all of these regions, the cloud of points representing the ensemble spread for near-term trends is shifting away from the pre-industrial ellipses[17]. Differences between scenarios can be seen, but they are small compared to the size of internal variability. Indeed, trends of the opposite sign to the ensemble means are quite common for some ensemble members for Rx5day over the next 20 years, and cooling trends for TXx are also seen in some members. Broadly consistent results for other models are shown in Figure S6-8.

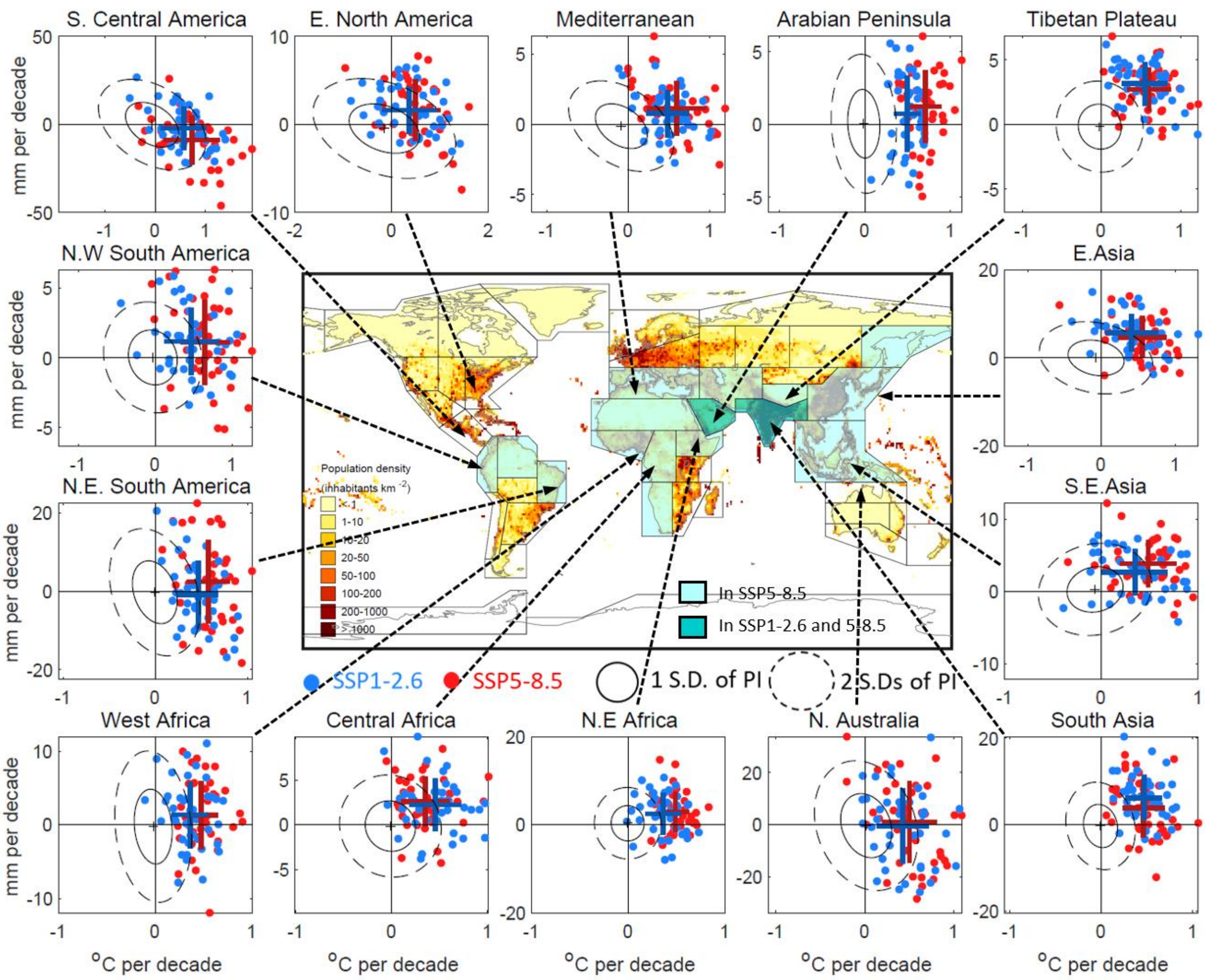

Figure 2: Regional joint near-term trends in TXx and Rx5day: The central map highlights the regions that show an ensemble mean combined rate of change of TXx and Rx5day for 2021-2040 that is more than 2 standard deviations of variability in pre-industrial 20-year rates of change in at least 3 out of 4 models (see Methods) in SSP5-8.5 (light turquoise shading) and both SSP1-2.6 and 5-8.5 (dark turquoise shading). Population density for 2020 from the GPWv4 dataset[18] is shown with red shading. Scatterplots show, for selected regions, the trend in TXx (x-axes) vs Rx5day (y-axes) per decade for 2021-2040 for each ensemble member (dots), and their ensemble mean trend and standard deviation spread (crosses) for SSP1-2.6 (blue) and SSP5-8.5 (red) based on the ACCESS-ESM1-5 ensemble. Ellipses show confidence regions

for pre-industrial variability of 20-year trends: solid for the 40th percentile confidence ellipse (corresponding to approximately 1 standard deviation) and dashed for 86.5th percentile ellipse (~2 standard deviations, see Methods). The ensemble mean PI trend is indicated with a small black cross.

Figure 3a-b shows the full spatial patterns of near-term joint TXx and Rx5day rates of change for the ACCESS-ESM1-5 ensemble mean. Combined changes exceed 2 or even 2.5 standard deviations in much of Northern Africa and the Arabian Peninsula, and parts of N.E. South America, Eastern Africa and the Tibetan Plateau under SSP5-8.5. There are also combined rates of change between 1-2 standard deviations over much of northern South America, southern Africa, southern Asia, Western Australia and some parts of North America and Northern Asia. Under SSP1-2.6 changes are more muted but still exceed 1 standard deviation over many low latitude locations. Results are similar for the other models (Figure S9), albeit weaker in MPI-ESM1-2-LR.

Figure 3 c-h shows regions with ensemble mean changes in rates exceeding 1 or 2 standard deviations of pre-industrial trend variability in at least 3 of 4 models, for joint changes, and also each index separately. Most land regions experience joint rates of change >1 S.D. in both scenarios, and a large part of the tropics and subtropics experience joint rates >2 S.D.s under SSP5-8.5, but also under SSP1-2.6 for south Asia and the Arabian Peninsula. Almost all regions also experience changes in rates of TXx >1 S.D. in at least one scenario, and parts of Africa, northern South America, Western central Asia, the Arabian Peninsula and southern Europe experience changes >2 S.D.s. These latter are regions with low trend variability (Figure S17) and also correspond well to the regions experiencing the earliest emergence of (absolute) mean and extreme temperature changes from interannual variability[19–23]. Fewer regions experience large changes in rates for Rx5day, but nevertheless, changes greater than 1 S.D. are seen in most high latitude regions in the northern hemisphere, and also in equatorial Africa and southern and eastern Asia. Central Africa is the only region surpassing 2 S.D.s for Rx5day. Again, this pattern reflects that of earliest mean and extreme precipitation emergence[20,24,25]. Results for individual models can be seen in Figure S4.

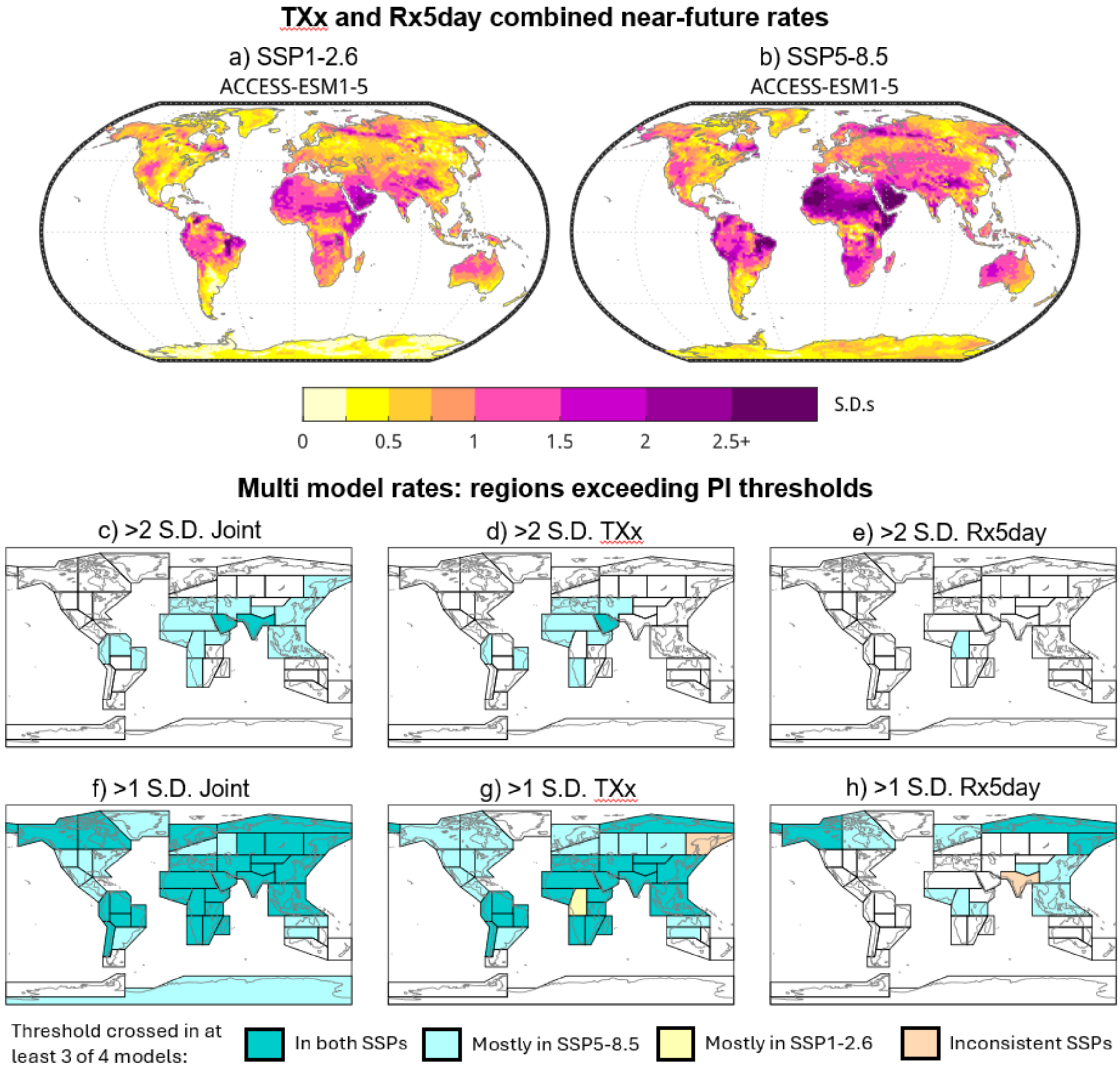

Figure 3: Spatial patterns of near-term joint rates of change in extremes, and their components. Top row: ACCESS-ESM1-5 ensemble mean combined near-term rates of change

for TXx and Rx5day expressed in standard deviations of pre-industrial variability of trends, a) for SSP1-2.6, and b) for SSP5-8.5. (c-h) Regions with near-term ensemble mean rates of change greater than 2 (c-e), and 1 (f-h) standard deviations of pre-industrial variability in 20-year trends in at least 3 of 4 models. Panels c and f are for both indices combined (as in Figure 2), whilst d+g is for TXx and e+h for Rx5day. Shading colour indicates which scenario(s) the threshold is crossed in (see Methods for details).

Population affected

In Table 1 we show the percentage of global population affected by near-term rates of change larger than 2, 1.5 and 1 standard deviation of pre-industrial variability in 20-year trends, which we define here as unprecedented, highly unusual and unusual respectively. Population affected is taken as the sum of (present-day, land-based) population in regions where 3 or more models show ensemble mean changes in rates passing these thresholds (Methods).

% world pop.	**Joint Changes**		**TXx**		**Rx5day**	
affected	**ssp126**	**ssp585**	**ssp126**	**ssp585**	**ssp126**	**ssp585**
>2 S.D.	19.9	68.8	0.9	20.9	0.0	1.7
>1.5 S.D.	59.9	83.3	37.5	72.9	0.0	6.5
>1 S.D.	76.9	90.5	74.5	88.8	19.2	55.9

Table 1: Percentage of the world's population affected by strong rates of change of climate extremes in the next 20 years: The proportion of global population that will experience near-term (2021-2040) rates of change larger than 2 ("unprecedented"), 1.5 ("highly unusual") and 1 ("unusual") standard deviations of pre-industrial variability in 20-year trends, based on the regions highlighted in Figure 3c-h and S3.

Under SSP5-8.5, almost 70% of the world's current population will experience unprecedented joint rates of change of both indices combined, 83% very unusual and 91% unusual. Even under strong mitigation (SSP1-2.6) 20% of the world's population will experience joint rates larger than 2 S.D.s of PI trends, 60% >1.5 S.D.s, and 77% >1 S.D. A large proportion of population will experience unprecedented (21%), highly unusual (73%) or unusual (89%) rates of change in temperature extremes under SSP5-8.5. This proportion reduces under strong mitigation, but still reaches 38% and 75% for highly unusual and unusual rates of change, respectively. Finally, a smaller proportion of global population will be affected by large changes in rates for precipitation extremes given their higher variability compared to forced changes, but nevertheless 56% of people will experience rates >1 S.D. of pre-industrial rates under SSP5-8.5 and 19% under SSP1-2.6.

The reason that more people are affected by large changes in joint rates than might be expected from individual changes in TXx and Rx5day, is that to exceed e.g. 2 S.D.s for joint changes, both individual indices would only need to change by 1.4 S.D.s each (see Methods). When very populous regions, e.g. South Asia or East Asia cross a threshold, this makes a large difference to the population affected.

Rates beyond 2040, and the influence of aerosol cleanup

We have also investigated the continued evolution of regional rates of change beyond 2040, and the potential influences of strong near-term reductions in aerosol emissions. Both are shown in detail in the Supplementary Information. As expected, rates of change remain high throughout the 21st century under SSP5-8.5, while they broadly decline in SSP1-2.6 and are largely consistent with preindustrial rates by 2080 (Figures S10-S13). However, even under very strong emissions mitigation and Paris-compatible global warming, we find regions of strong forced rates of change of extreme events until 2060, particularly for warm extremes. Further studies of rates of change, up to and after stabilization of global warming, are therefore warranted. For aerosols, we exploit the fact that over the period 2021-2040, SSP1-2.6 and SSP3-7.0 have only moderately different greenhouse gas concentration trends (Figure S14) but marked differences in aerosol trends, predominantly over Asia. While results are mixed, we do find that aerosol cleanup is associated with an enhanced increase in the warmest days in both summer and winter months over parts of Southern and Eastern Asia, accompanied by a wintertime (DJF) wetting (Figure S15). These results are consistent with the expected influence of a loss of regional, near-source aerosol induced surface cooling. Effects on Asian summer monsoon precipitation were mixed, with two models (ACCESS-ESM1-5 and MPI-ESM1-2-LR) showing statistically significant enhanced monsoon season wet extreme rates.

Discussion

The present analysis is based primarily on large ensembles of climate model simulations, which allow us to explore the role of internal variability, whilst also being able to pin down the models' forced response. This depends, however, on the models being able to realistically simulate decadal rates of change, and their responses to climate forcing. Overall, for the ensemble means we find a robust evolution of both hot and wet extremes across the four models studied, albeit with regional differences consistent with known biases such as monsoon climatologies (Wilcox et al. 2020), and response strengths broadly in line with modelled Equilibrium Climate Sensitivities, particularly for TXx. When looking at individual realizations there is substantial variability in regional rates of change, even on 20-year timescales, including uncertainty in the sign of the trends. While a lack of pre-industrial observations makes characterizing unprecedented rates of change in climate extremes challenging, large ensembles do indicate how rates of change will likely change between the pre-industrial period and the present day. As our main process of interest here is the internal variability that leads to decadal scale rates of change (and its interactions with forced changes) we have primarily evaluated model performance against this metric (Supplementary Figures S18). Daily precipitation information is unfortunately sparse in many regions, and the short observational record does not allow a large sample of short-term trend periods. However, for TXx, modelled 20-year trend variability is consistent with observational estimates for the majority of regions. For Rx5day it is well represented in ACCESS-ESM1-5 and CanESM5, especially in the key regions shown in Figures 1-2, but is underestimated in a number of regions in EC-Earth3 and MPI-ESM1-2-LR. Underestimated trend variability may be related to underestimated climatological mean Rx5day, with possible consequences for the size of forced trends (see discussion in supplement), but is unlikely to influence our key results. Assessing whether models are fit-for-purpose for projecting decadal rates of change is clearly a remaining challenge, which cannot be fully resolved with currently available datasets. For the analysis presented here, our overall conclusions of rapid near-term rates of change in major populated regions are generally supported by an agreement between models, observations and reanalysis.

Climate models can also have deficiencies in representing processes such as convective extreme precipitation, which must be parameterized at these resolutions, or mean-state biases. By using four different models we capture some inter-model uncertainty, although this small sample will not fully reflect model uncertainty across CMIP6. The sample of models used include ones that have high climate sensitivities relative to the IPCC likely range (Methods) which may lead to stronger rates for these particular models (see also Smith et al, 2015[4]; Chavaillaz et al., 2016[15]) . There is, however, no a priori reason to exclude so-called "hot models" for regional trend analyses, so we do not perform a model selection or weighting of their results here.

Whilst over large parts of the globe, these four models agree on the patterns of changes, if not the magnitude, there are regions where Rx5day or CDD are of opposite sign in different models, consistent with greater model uncertainties in projections of precipitation-related quantities than temperature-related ones found in previous studies[11,26,27]. These differences all constitute uncertainties that should be borne in mind when considering the results of this study.

Another caveat is our usage of global, coarse-resolution models, and large geographical regions. These do not capture the full spatial patterns of trends, for which regional, high-resolution modelling would be useful. However, current regional climate models have no, or only rudimentary, treatment of aerosols, and which influences rates-of-change of extreme events both directly and indirectly[28,29]. Further, the indices used in the present analysis (TXx, Rx5day, CDD) are useful, but not necessarily the most impact relevant in all regions. Further work is critically needed on regional rates-of-change of extremes using updated regional models, and locally adapted, multi-hazard indicators.

We find that over the coming decades, regional trends in extreme weather well beyond internal variability are likely in many regions, affecting a large fraction of global population, even under strong emissions mitigation. These conclusions emphasize the need for both continued mitigation and adaptation to potentially unprecedented changes over the next 20 years even under a low emissions scenario.

Corresponding author

Correspondence should be addressed to Carley Iles: carley.iles@cicero.oslo.no

Acknowledgements

This research has received funding from the European Union's Horizon 2020 research and innovation programme under grant agreements No 101003826 through the CRiceS project and No 820655 through the EXHAUSTION project and also from the Norwegian Research Council through the projects CATHY (324182) and QUISARC (248834). We acknowledge the Centre for Advanced Study in Oslo, Norway that funded and hosted our HETCLIF centre during the academic year of 2023/24. We acknowledge the World Climate Research Programme, which, through its Working Group on Coupled Modelling, coordinated and promoted CMIP6. We thank the climate modelling groups for producing and making available their model output, the Earth System Grid Federation (ESGF) for archiving the data and providing access, and the multiple funding agencies who support CMIP6 and ESGF.

Author Contributions

CI and BHS conceived and designed the experiments, CI performed the experiments and analysed the data, MS contributed materials/analysis tools, all authors wrote the paper.

References

1. IPCC. Summary for Policymakers. in *Climate Change 2021: The Physical Science Basis. Contribution of Working Group I to the Sixth Assessment Report of the Intergovernmental Panel on Climate Change* (eds. Masson-Delmotte, V. et al.) 3−32 (Cambridge University Press, 2021). doi:10.1017/9781009157896.001.

2. Gulev, S. K. *et al.* Changing State of the Climate System. in *Climate Change 2021: The Physical Science Basis. Contribution of Working Group I to the Sixth Assessment Report of the Intergovernmental Panel on Climate Change* (eds. Masson-Delmotte, V. et al.) 287–422 (Cambridge University Press, 2021). doi:10.1017/9781009157896.004.

3. Samset, B. H. *et al.* Steady global surface warming from 1973 to 2022 but increased warming rate after 1990. *Commun. Earth Environ.* **4**, 400 (2023).

4. Smith, S. J., Edmonds, J., Hartin, C. A., Mundra, A. & Calvin, K. Near-term acceleration in the rate of temperature change. *Nat. Clim. Chang.* **5**, 333–336 (2015).

5. Loarie, S. R. *et al.* The velocity of climate change. *Nature* **462**, 1052–1055 (2009).

6. O'Neill, B. C. & Oppenheimer, M. Climate change impacts are sensitive to the concentration stabilization path. *Proc. Natl. Acad. Sci.* **101**, 16411–16416 (2004).

7. Fischer, E. M., Sippel, S. & Knutti, R. Increasing probability of record-shattering climate extremes. *Nat. Clim. Chang.* **11**, 689–695 (2021).

8. Philip, S. Y. *et al.* Rapid attribution analysis of the extraordinary heat wave on the Pacific coast of the US and Canada in June 2021. *Earth Syst. Dyn.* **13**, 1689–1713

(2022).

9. Ranasinghe, R. *et al.* Climate Change Information for Regional Impact and for Risk Assessment. in *Climate Change 2021: The Physical Science Basis. Contribution of Working Group I to the Sixth Assessment Report of the Intergovernmental Panel on Climate Change* (eds. Masson-Delmotte, V. et al.) 1767–1926 (Cambridge University Press, 2021). doi:10.1017/9781009157896.014.

10. Zscheischler, J. *et al.* Future climate risk from compound events. *Nat. Clim. Chang.* **8**, 469–477 (2018).

11. Seneviratne, S. I. *et al.* Weather and Climate Extreme Events in a Changing Climate. in *Climate Change 2021: The Physical Science Basis. Contribution of Working Group I to the Sixth Assessment Report of the Intergovernmental Panel on Climate Change* (eds. Masson-Delmotte, V. et al.) 1513–1766 (Cambridge University Press, 2021). doi:10.1017/9781009157896.013.

12. IPCC. *Climate Change 2021: The Physical Science Basis. Contribution of Working Group I to the Sixth Assessment Report of the Intergovernmental Panel on Climate Change*. (Cambridge University Press, 2021). doi:10.1017/9781009157896.

13. Sedláček, J. & Knutti, R. Half of the world's population experience robust changes in the water cycle for a 2 °C warmer world. *Environ. Res. Lett.* **9**, 044008 (2014).

14. Lehner, F. & Stocker, T. F. From local perception to global perspective. *Nat. Clim. Chang.* **5**, 731–734 (2015).

15. Chavaillaz, Y., Joussaume, S., Dehecq, A., Braconnot, P. & Vautard, R. Investigating the pace of temperature change and its implications over the twenty-first century. *Clim.*

Change **137**, 187–200 (2016).

16. Iturbide, M. *et al.* An update of IPCC climate reference regions for subcontinental analysis of climate model data: definition and aggregated datasets. *Earth Syst. Sci. Data* **12**, 2959–2970 (2020).

17. Sanderson, B. M., Oleson, K. W., Strand, W. G., Lehner, F. & O’Neill, B. C. A new ensemble of GCM simulations to assess avoided impacts in a climate mitigation scenario. *Clim. Change* **146**, 303–318 (2018).

18. Center for International Earth Science Information Network-CIESIN-Columbia University. Gridded Population of the World, Version 4 (GPWv4): Population Density Adjusted to Match 2015 Revision UN WPP Country Totals, Revision 11. (2018) doi:https://doi.org/10.7927/H4F47M65.

19. Hawkins, E. & Sutton, R. Time of emergence of climate signals. *Geophys. Res. Lett.* **39**, L01702 (2012).

20. King, A. D. *et al.* The timing of anthropogenic emergence in simulated climate extremes. *Environ. Res. Lett.* **10**, 094015 (2015).

21. Diffenbaugh, N. S. & Scherer, M. Observational and model evidence of global emergence of permanent, unprecedented heat in the 20th and 21st centuries. *Clim. Change* **107**, 615–624 (2011).

22. Chen, D. *et al.* Framing, Context, and Methods. in *Climate Change 2021: The Physical Science Basis. Contribution of Working Group I to the Sixth Assessment Report of the Intergovernmental Panel on Climate Change* (eds. Masson-Delmotte, V. et al.) 147–286 (Cambridge University Press, 2021). doi:10.1017/9781009157896.003.

23. Mahlstein, I., Knutti, R., Solomon, S. & Portmann, R. W. Early onset of significant local warming in low latitude countries. *Environ. Res. Lett.* **6**, 034009 (2011).

24. Nguyen, T.-H., Min, S.-K., Paik, S. & Lee, D. Time of emergence in regional precipitation changes: an updated assessment using the CMIP5 multi-model ensemble. *Clim. Dyn.* **51**, 3179–3193 (2018).

25. Mahlstein, I., Portmann, R. W., Daniel, J. S., Solomon, S. & Knutti, R. Perceptible changes in regional precipitation in a future climate. *Geophys. Res. Lett.* **39**, (2012).

26. Hawkins, E. & Sutton, R. The potential to narrow uncertainty in projections of regional precipitation change. *Clim. Dyn.* **37**, 407–418 (2011).

27. Lehner, F. *et al.* Partitioning climate projection uncertainty with multiple large ensembles and CMIP5/6. *Earth Syst. Dyn.* **11**, 491–508 (2020).

28. Persad, G. *et al.* Rapidly evolving aerosol emissions are a dangerous omission from near-term climate risk assessments. *Environ. Res. Clim.* **2**, 032001 (2023).

29. Schumacher, D. L. *et al.* Exacerbated summer European warming not captured by climate models neglecting long-term aerosol changes. *Commun. Earth Environ.* **5**, 182 (2024).

Online Methods

Climate model simulations

We analyse four large ensembles of climate model simulations produced as part of the CMIP6 exercise[30]: ACCESS-ESM1-5 (40 members[31]), MPI-ESM1-2-LR (30[32]), CanESM5 (50[33]) and EC-Earth3 (57; 20 for the preindustrial case[34,35]). See Table S1 for details. The equilibrium climate sensitivities (ECS) of these models range from the IPCC AR6 best estimate (MPI-ESM1-2-LR; 3.0°C for a doubling of CO_2 concentrations), to a value at the upper end of the CMIP6 range (CanESM5; 5.6°C)[1,36]. ACCESS-ESM1-5 has an ECS of 3.9°C, EC-Earth3 has 4.3°C. The IPCC likely range is 2.5-4°C and very likely range 2-5°C.

We use the historical CMIP6 simulations for the pre-industrial period, and the future scenarios SSP1-2.6, SSP5-8.5 and SSP3-7.0. The historical simulations are forced with observed records of both anthropogenic and natural forcing agents, including greenhouse gases, anthropogenic aerosols, volcanic aerosols, solar variability and land-use change[30]. The future scenarios include various possible trajectories of greenhouse gas emissions, land use and aerosols[37]. To assess the influence of emissions trajectories on trends over the coming 20 years, we contrast a very low (SSP1-2.6) and very high (SSP5-8.5) greenhouse gas emissions scenario. When examining trends related to aerosol clean-up, we contrast SSP1-2.6 with SSP3-7.0, the former having rapid aerosol reductions over the next 20 years, notably from India and China, and the latter having continued growth of emissions (see Figure S14).

We use ACCESS-ESM1-5 as an example model in the main text, since it has a climate sensitivity consistent with recent assessments, and middle of the range results compared to the other models, as well as reasonable trend variability compared to ERA5 (Supplementary Material).

The other models are fully presented in the supplement. Multi-model results are based on all four models, as described below.

Extreme event indices

We analyse regional trends in two widely used climate extremes indices that form part of the Expert Team on Climate Change Detection and Indices (ETCCDI) set of indices[38]: The annual maximum of daily maximum temperatures (TXx), as a measure of heat extremes, and the total precipitation falling in the wettest 5 consecutive day period of the year (Rx5day) as a measure of wet extremes. We also present further analysis for dry extremes in the supplement, for the maximum number of consecutive dry days per year (CDD). We use a version where the dry spell is not allowed to continue past the year boundary, i.e. the maximum value is 365 days per year.

Near-term and preindustrial trends

We calculate trends over the period 2021-2040, defined here as the “near-term”, using a linear regression of yearly ETCCDI index values for each model ensemble member. For regional results we calculate the regional-mean land-only time series first and then calculate trends, whilst for spatial plots trends are calculated per grid cell. We also calculate 20-year trends for the preindustrial (PI) period by examining 20-year periods within the time frame 1850-1900, shifting the start year by 5 years each time. This yields a total sample size of 7x 20-year trends per ensemble member. This method was chosen to avoid trends driven by the effect of volcanic eruptions overly influencing the PI trends (see Figure S16).

Combined rates of change

As well as near-term rates of change for the separate extreme indices, we examine joint rates of change in TXx and Rx5day, to identify regions subject to multiple stressors at the same time.

In order to relate changes to preindustrial variability of 20-year trends, we convert changes in both indices to units of standard deviations of their PI trend variability. We then define a combined trend as the sum of squares of the two metric trends:

$$Combined\ trend = \sqrt{\left(\frac{R_{TXx}^{near-term} - R_{TXx}^{PI}}{\sigma(r_{TXx}^{PI})}\right)^2 + \left(\frac{R_{Rx5day}^{near-term} - R_{Rx5day}^{PI}}{\sigma(r_{Rx5day}^{PI})}\right)^2}$$

Here, r_x^y is the 20-year rate-of-change in a single ensemble member, for indicator x in period y (near-term future or preindustrial (PI)), R_x^y is the corresponding ensemble mean, and σ is the standard deviation across all ensemble members.

As an example, if both indices exhibit an increase in the ensemble mean rate of change between the near-term and PI that is 1 standard deviation of the PI variability of trends, then the combined trend will be 1.4.

Evaluation against observational datasets

To assess the representation of 20-year trend variability in the climate models used for this study, we perform a regional comparison with the ERA5 reanalysis[39] for TXx and Rx5day, and additionally the Rainfall Estimates on a Gridded Network (REGEN) daily gauge-based dataset for Rx5day[40]. ERA5 temperature and precipitation data were available for the period 1941-2022 on a 0.25°grid, whilst REGEN is available from 1950-2016 on a 1°grid. REGEN combines stations from the Global Precipitation Climatology Centre (GPCC)[41], Global Historical Climatology Network – Daily (GHCN-daily)[42] and other sources, and is available as two versions: REGEN-LONG, which includes only stations with at least 40 years of data, and REGEN-

ALL, which includes a much larger number of stations. Each is spatially interpolated and comes with a data quality mask. TXx and Rx5day were calculated in the same way as for the climate model data. The results of the evaluation are presented in the Supplementary Materials (Figures S18).

Region selection

We calculate regional results for the 46 land regions defined as part of the IPCC sixth assessment cycle[16], with a further masking applied to retain only grid cells with >50% land. These regions are widely used for climate studies and are a refined version of those used in previous IPCC cycles. They are defined with climate homogeneity in mind, both in terms of historical mean climate and projections, whilst also being large enough to be appropriate for use with the CMIP6 generation of models, at around 1 degree resolution.

Where a sub-selection of regions is shown, e.g. in Figures 1 and 2, these are subjectively chosen based on a combination of 1) showing a clear shift in the distribution of trends away from the pre-industrial equivalent, 2) prioritising regions with high population density and 3) representing all continents where we find clear changes. More specifically, for combined rates of change, and for TXx point 1) is based on regions undergoing an ensemble mean rate at least 1.5 standard deviations bigger than the PI equivalent in at least three models (as seen in Figures 3 and S3), whilst for Rx5day, where changes are less clear relative to PI due to higher intrinsic variability, we use a lower threshold of 1 standard deviation. Results for remaining regions are shown in the supplement.

Colour coding of SSPs in multi-model regional map figures

In Figures 2, 3, S3 and S4, regions are colour coded according to the SSP in which a given threshold is crossed. The thresholds are defined as when the change in ensemble mean rates between the PI and near-term is greater than the PI 20-year trend variability by a certain number of standard deviations.

Two SSPs are examined (SSP1-2.6 and SSP5-8.5). For single model plots there are thus four options for threshold crossing: In either SSP5-8.5, or SSP1-2.6, or both, or none. For the multi model plots, we use the following colour coding:

1) The given threshold must be passed in at least 3 of 4 models for a colour to be assigned.

2) The colour categories are then as follows:

- "In both SSPs" (teal)- at least 3 models cross the threshold for both SSPs (this includes situations where 3 models cross the threshold in both SSPs, and the last model crosses for only one SSP)
- "Mostly in SSP5-8.5" (light cyan)- More models cross the threshold for SSP5-8.5 than for SSP1-2.6
- "Mostly in SSP1-2.6" (yellow)- More models cross the threshold for SSP1-2.6 than for SSP5-8.5
- Inconsistent SSPs (orange)- any combination that does not fit into the previous categories e.g. two models only cross the threshold in SSP5-8.5 and the other two only for SSP1-2.6, or 1 model only SSP5-8.5, another only SSP1-2.6 and the remaining two both SSPs.

Population calculations

Population density and totals for the year 2020 are taken from the United Nations World Population Prospects Gridded Population of the World, Adjusted Version 4 dataset, on a 1 degree grid[18,43]. Whilst population will change over the next 20 years, some of the regions with the clearest acceleration in rates of change are also those where population is projected to increase fastest e.g. Africa, likely putting our results on the conservative side. When calculating the percentage of the global population affected by near-term rates of change in extreme indices greater than a given threshold of preindustrial variability of 20-year trends, we sum up the populations in the AR6 WG1 regions affected by such changes as shown in Figure 3c-f and S3. These are regions where 3 out of 4 large ensembles show ensemble mean changes in rates passing these thresholds. For SSP5-8.5 estimates we include teal, light cyan and orange regions (i.e. threshold is crossed mostly in SSP5-8.5, both SSPs and inconsistent SSPs respectively- see previous section), and for SSP1-2-6 teal, yellow and orange regions (both SSPs, mostly SSP1-2.6 and inconsistent SSPs respectively).

Since the climate data are masked to land only, we also mask population data to land only when calculating the total population affected. This means that 90.8% of the world's population is considered in our analysis. Population affected is then expressed as a percentage of total global unmasked population. This means that our population affected estimates are on the conservative side, since we cannot say anything about the remaining population, for example in some small islands.

Statistical Testing

We use a two-sample Kolmogorov Smirnov test (K-S test) to test whether the differences between empirical distributions of 20-year trends between two periods or two scenarios from a given climate model ensemble are statistically significant at the 5% significance level. The K-S test is a non-parametric test which compares two samples and tries to determine whether these come from the same underlying continuous distribution by examining the maximum distance between the empirical distribution functions based on the two samples. For this test, the underlying distribution does not have to be specified or even known and it takes both location and shape of the distribution into account.

Ellipses

The ellipses shown in Figures 2, S5-8 and S19-22 correspond to the area covered by the 40th and 86.5th percentiles of the bivariate distributions of the 20-year trends in TXx vs Rx5day for the preindustrial period, estimated from their respective covariance matrices. This corresponds approximately to one and two standard deviations, respectively, of the chi-squared distribution generated from the sum of the squared components of the bivariate distribution.

Data availability

The climate model data used for this analysis are publicly available from the ESGF portals e.g. https://esgf-data.dkrz.de/search/cmip6-dkrz/. ETCCDI indices for CMIP6 models are available from the Copernicus Climate Data Store at https://cds.climate.copernicus.eu/cdsapp#!/dataset/sis-extreme-indices-cmip6?tab=overview. ERA5 temperature and precipitation data are available from https://cds.climate.copernicus.eu/cdsapp#!/dataset/reanalysis-era5-single-levels?tab=overview. REGEN-LONG is available from https://zenodo.org/records/4922162 and REGEN-ALL from https://zenodo.org/records/4922160. Population data are available from https://sedac.ciesin.columbia.edu/data/collection/gpw-v4.

Code availability

The code used in this analysis will be deposited in a publicly accessible archive and made available upon publication of this manuscript.

Methods References

30. Eyring, V. *et al.* Overview of the Coupled Model Intercomparison Project Phase 6 (CMIP6) experimental design and organization. *Geosci. Model Dev.* **9**, 1937–1958 (2016).

31. Mackallah, C. *et al.* ACCESS datasets for CMIP6: methodology and idealised experiments. *J. South. Hemisph. Earth Syst. Sci.* **72**, 93–116 (2022).

32. Mauritsen, T. *et al.* Developments in the MPI-M Earth System Model version 1.2 (MPI-ESM1.2) and Its Response to Increasing CO2. *J. Adv. Model. Earth Syst.* **11**, 998–1038 (2019).

33. Swart, N. C. *et al.* CCCma CanESM5 model output prepared for CMIP6 CMIP historical. (2019) doi:10.22033/ESGF/CMIP6.3610.

34. Döscher, R. *et al.* The EC-Earth3 Earth system model for the Coupled Model Intercomparison Project 6. *Geosci. Model Dev.* **15**, 2973–3020 (2022).

35. Wyser, K. *et al.* The SMHI Large Ensemble (SMHI-LENS) with EC-Earth3.3.1. *Geosci. Model Dev.* **14**, 4781–4796 (2021).

36. Meehl, G. A. *et al.* Context for interpreting equilibrium climate sensitivity and transient climate response from the CMIP6 Earth system models. *Sci. Adv.* **6**, eaba1981 (2022).

37. O'Neill, B. C. *et al.* The Scenario Model Intercomparison Project (ScenarioMIP) for CMIP6. *Geosci. Model Dev.* **9**, 3461–3482 (2016).

38. Sillmann, J., Kharin, V. V., Zhang, X., Zwiers, F. W. & Bronaugh, D. Climate extremes indices in the CMIP5 multimodel ensemble: Part 1. Model evaluation in the present climate. *J. Geophys. Res. Atmos.* **118**, 1716–1733 (2013).

39. Hersbach, H. *et al.* The ERA5 global reanalysis. *Q. J. R. Meteorol. Soc.* **146**, 1999–2049 (2020).

40. Contractor, S. *et al.* Rainfall Estimates on a Gridded Network (REGEN) – a global land-based gridded dataset of daily precipitation from 1950 to 2016. *Hydrol. Earth Syst. Sci.* **24**, 919–943 (2020).

41. Ziese, M. *et al.* GPCC Full Data Daily Version.2018 at 1.0°: Daily Land-Surface Precipitation from Rain-Gauges built on GTS-based and Historic Data. (2018) doi:10.5676/DWD_GPCC/FD_D_V2018_100.

42. Menne, M. J., Durre, I., Vose, R. S., Gleason, B. E. & Houston, T. G. An Overview of the Global Historical Climatology Network-Daily Database. *J. Atmos. Ocean. Technol.* **29**, 897–910 (2012).

43. Center for International Earth Science Information Network-CIESIN-Columbia University. Gridded Population of the World, Version 4 (GPWv4): Population Count Adjusted to Match 2015 Revision of UN WPP Country Totals, Revision 11. (2018) doi:https://doi.org/10.7927/H4PN93PB.